Available online at www.sciencedirect.com

SCIENCE DIRECT

Thin Solid Films 467 (2004) 36–42

www.elsevier.com/locate/tsf

Spectroscopic ellipsometry studies on the optical constants of indium tin oxide films deposited under various sputtering conditions

Yeon Sik Jung*

R&D Center, Samsung Corning, 644, Jinpyoung-dong, Gumi, Kyoung-buk 730-725, South Korea

Received 24 July 2003; received in revised form 2 February 2004; accepted 21 February 2004
Available online 28 March 2004

Abstract

In this research, ITO thin film samples were prepared under various DC magnetron sputtering conditions. Their optical constants were analyzed based on a model combining Drude and Lorentz oscillator terms. Lower amount of oxygen flow, moderate range of sputtering pressure, and higher deposition temperature resulted in lower refractive indices. It was revealed that the refractive indices of the films are closely related with their crystallographic orientations. The samples with higher refractive indices had more (222)-oriented crystallographic structures. In addition, based on X-ray diffraction (XRD) analyses, the difference in the refractive indices between bottom and upper layers was explained from graded crystallographic orientation. Extinction coefficients in the visible were closely related with the crystallinity of the films and their stoichiometry, and with carrier concentration measured by Hall effect in the near infrared.

Keywords: Indium tin oxide; Ellipsometry; Optical properties; Sputtering

1. Introduction

Tin-doped indium oxide (ITO) thin films have been commonly used for opto-electronic applications due to low resistivity, high transmittance, and good etching properties [1–3]. Many researchers have reported the use of spectroscopic ellipsometry for measuring optical constants (refractive index, n, and extinction coefficient, k) of ITO thin films [4–10]. Several dispersion relations such as the Cauchy models or the Lorentz oscillator models or the Drude models have been used to describe the optical constants of ITO thin films [6–10]. Graded structure of ITO thin films makes it difficult to get a good agreement between their measured and calculated Ψ and Δ spectra with a simple one-layer model [7]. Thus, several ways to describe the graded structure have been proposed. One is to assume a linear grade of the optical constants through the film depth using the effective medium approximation (EMA) [6,7,11]. However, in the cases of strong index gradient or films thicker than several tens of nanometers, it was recommended to split the film into multiple uniform films and to try to fit for the optical constants of each film [5].

DC magnetron sputtering deposition techniques have been commonly used to deposit ITO thin films of fine electrical and optical properties [12–14]. Furthermore, due to better productivity than other deposition methods, it is widely used for mass production process. However, there have not been sufficient discussions about the influence of DC magnetron sputtering parameters on the optical constants of ITO thin films. Fukarek and Kersten [15] have already reported the application of in situ ellipsometry to the monitoring of the deposition of ITO layers by reactive magnetron sputtering. They found that refractive index and deposition rate depend on discharge voltage and oxidation state of target. However, they employed a single-wave (λ=632.8 nm) ellipsometry, which is adequate for in situ measurement, but cannot provide spectroscopic data ranged from the visible to the infrared. Meanwhile, they used a metal alloy target for deposition, which is not adopted for the ITO films of high quality nowadays because of relatively unstable processes and properties. As a result, a practical reference

* Present address: Thin Film Materials Research Center, Korea Institute of Science and Technology, 39-1 Hawolgok-dong, Seongbuk-gu, Seoul 136-791, South Korea. Tel.: +82-2-958-5565; fax: +82-2-958-6851.
E-mail address: ysjung@kist.re.kr (Y.S. Jung).

0040-6090/$ - see front matter © 2004 Elsevier B.V. All rights reserved.
doi:10.1016/j.tsf.2004.02.047

with spectroscopic ellipsometry data of ITO films deposited with ITO oxide targets has not been given. Thus, in this research, spectroscopic ellipsometry with multiple measurement angles was employed to get the spectral optical constants of the ITO films deposited with an ITO oxide target under various sputtering conditions. The variation of the optical constants with different sputtering conditions is discussed in terms of the change in crystallographic orientations, degree of crystallinity and stoichiometry. In addition, the extinction coefficients in the near infrared region were correlated with the free electron concentration calculated by Hall measurement.

2. Experimental

2.1. Preparation of samples

ITO thin films were sputter-deposited using an ITO target in an in-line magnetron sputter-deposition system equipped with DC power suppliers. The chamber, which was equipped with a load-lock system and diffusion pumps, had a base pressure of 6×10^{-4} Pa. The target (128×450 mm) used was a sintered ITO containing 10 wt.% SnO_2 (99.99%). Sputtering was carried out at a pressure of 0.1–1.4 Pa in pure Ar or Ar/O_2 gas mixture with varying sputtering parameters such as sputtering pressure, oxygen flow rate and deposition temperature. The oxygen flow rate was from 0 to 3 sccm. The deposition temperature was usually 200 °C except the samples to investigate the effect of temperature. The films were deposited on p-type (100) Si wafers, which were placed 50 mm apart and parallel from the target surface. The substrates were cleaned in an ultrasonic bath containing a detergent (Deconex 12 PA) at 65 °C for 6 min, and then rinsed in deionized water in the ultrasonic bath for another 15 min. The cleaned substrates were dried at 100 °C for 15 min. The target was pre-sputtered for 3 min to remove the contaminants on surface and to stabilize the temperature of the target. The thickness of the films was about 150 nm. More specific deposition conditions and the electrical and structural properties were shown in Table 1.

Table 1
Deposition conditions of the ITO thin film samples and their electrical and structural properties

No.	Ar (sccm)	O_2 (sccm)	Pressure (Pa)	T_{sub} (°C)	Electrical properties		(222) [a] Peak ratio	Density (g/cm^3)
					μ (cm^2/V s)	N (10^{20} cm^{-3})		
1	12	–	0.10	200	19.4	7.12	0.701	7.05
2	20	–	0.15	200	22.1	8.54	0.655	7.12
3	60	–	0.70	200	21.1	9.21	0.530	7.12
4	200	–	1.4	200	20.6	7.95	0.636	6.65
5	20	1	0.15	200	25.4	7.93	0.71	7.25
6	20	3	0.15	200	37.6	4.05	1.0	6.94
7	20	–	0.15	50	20.3	4.95	1.0	7.01
8	20	–	0.15	100	24.4	6.03	1.0	7.08
9	20	–	0.15	350	29.9	10.2	0.312	7.34

[a] Relative (222)-peak intensity is $I_{(222)}/(I_{(222)}+I_{(400)})$ from XRD data.

2.2. Data analysis

From a Lorentz oscillator model, the complex dielectric function can be expressed like the following [7]:

$$\varepsilon(E) = \varepsilon(\infty) + \sum_{i=1}^{N} \frac{A_i}{E_i^2 - E^2 - i\Gamma_i E} \quad (1)$$

where $\varepsilon(E)$ is the complex dielectric function as a function of photon energy, $\varepsilon(\infty)$ is the dielectric function at infinite energy, A_i is the amplitude, Γ_i is the broadening, and E_i is the center energy of ith oscillator, respectively [7]. The four terms ($\varepsilon(\infty)$, A_i, Γ_i, and E_i) were used as fit parameters. The center energy of the first oscillator was fixed as 0 to describe free carriers based on the Drude model.

Ψ and Δ spectra were acquired using a spectroscopic ellipsometer (J.A. Woollam, VASE®) [4,7]. The measurement was conducted in the spectral range of 300–1000 nm at three angles of incidence (65°, 70°, and 75°) in steps of 10 nm. Acquiring the data further into infrared out to 2000 nm might be better for describing Drude absorption, however, because of the limitation of the facility, it was not possible to obtain ellipsometric data at above 1200 nm. The analysis of optical constants was based on the model shown in Fig. 1(c). A SiO_2 interfacial layer with the thickness of 2 nm, which was obtained by measuring bare Si wafers, was inserted in the model to improve the quality of fit. The optical constants of the ITO layers were analyzed based on a model combining a Drude absorption edge and Lorentz oscillators. To analyze the graded structure of the films, two independent layers were used. The thickness of the lower layers was fixed as 30 nm since the initial atomic layers of a few tens of nanometers have quite disordered microstructure. The cross-sectional SEM and TEM images of ITO films often show relatively porous and disordered initial layers of 20×30 nm, which may be due to island-type growth mode. The quality of fit, which was estimated by the mean square deviation, was lowest when the thickness of the lower layers were fixed as about 30 nm. The oscillator model parameters of the lower layers were being fit simultaneously with those of the upper layers, while those of SiO_2 interfacial layer were fixed. Surface roughness layer was modeled with the Bruggeman effective medium approximation (BEMA), where the mixture of 50% upper ITO film and 50% voids are assumed. The thickness of the BEMA layer was also declared as a fit parameter. Several times, it was confirmed that the fitting results were unique, reproducible and physically reasonable. To investigate the crystallographic orientation of the samples, conventional θ–2θ X-ray diffraction (XRD)

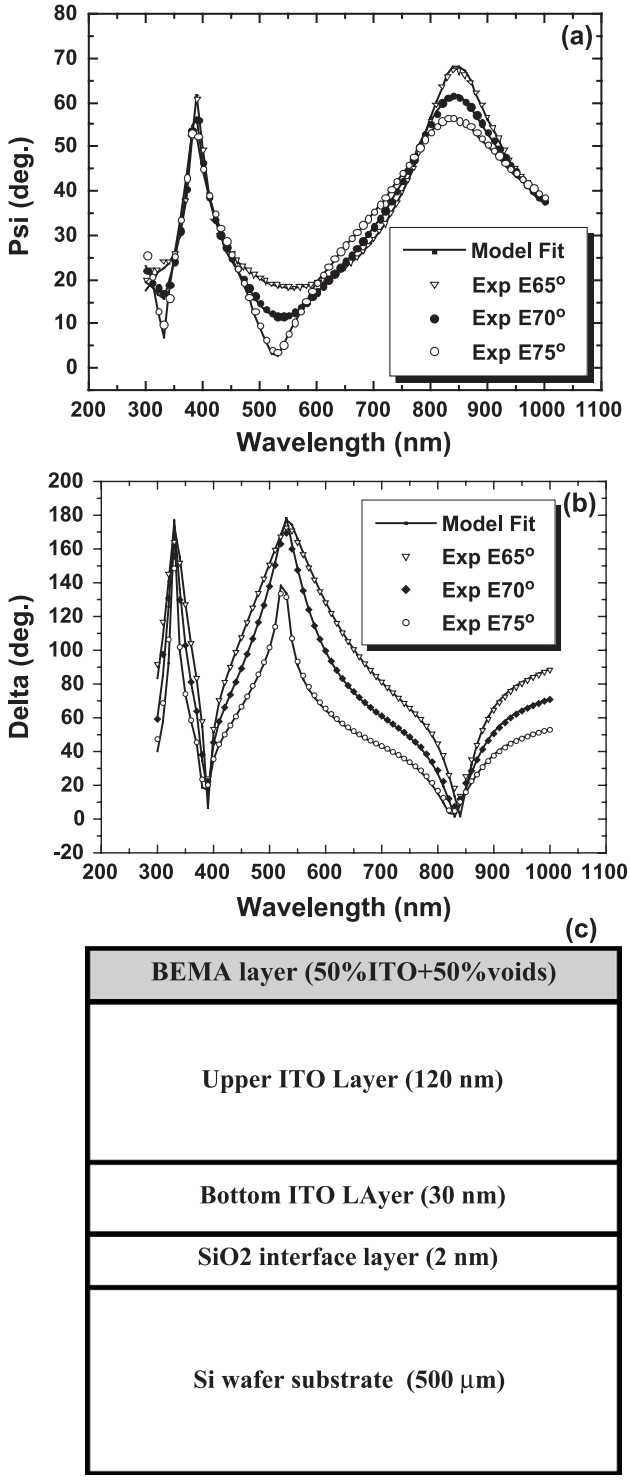

Fig. 1. Calculated and measured spectra of (a) Ψ and (b) Δ. (c) Four-layer model for data analyzing.

studies on the films were carried out in a Philips PW1710 diffractometer using Cu Kα radiation. Film density was measured by X-ray reflectometry (D8DISCOVER, Bruker) technique. The concentration and the mobility of electrons were measured using Hall effect and Van der Pauw's technique with magnetic field of 0.320 T.

3. Results and discussions

Fig. 1(a) and (b) shows the measured and the calculated Ψ and Δ spectra. The graphs show reasonably good agreement between the data throughout the measurement range. Thus, the mean square deviation between the data was sufficiently low.

Fig. 2(a) and (b) presents the spectra of the refractive indices and the extinction coefficients of the ITO films deposited at 200 °C and 0.15 Pa with different oxygen flow rate (sample numbers 2, 5, and 6). The compared optical constants were extracted from the upper ITO layer for all the samples. Within the oxygen gas flow range of this experiment, more oxygen flow resulted in higher refractive indices and lower extinction coefficients. Table 1 shows that higher oxygen flow rate leads to lower electron concentration and higher relative (222)-peak intensity (sample numbers 4, 5, and 6). The XRD profiles of the films were not directly presented, but showed mainly (222) and (400) peaks in the measurement range of 2θ=20–45°. The intensity of each peak was measured by fitting and integrating a Gaussian function.

The variation in optical constants of the ITO films deposited at different temperatures is shown in Fig. 3 (sample numbers 2, 7, 8, and 9). The deposition pressure was 0.15 Pa, and no additional oxygen gas was supplied.

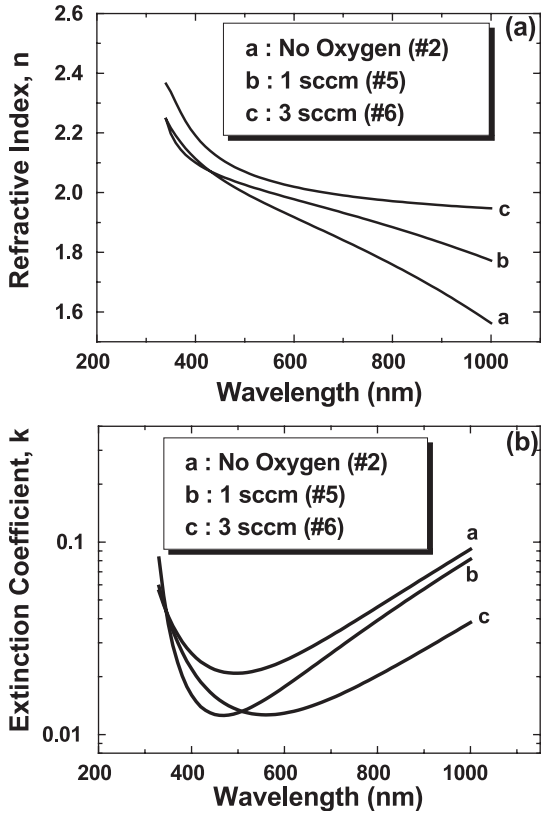

Fig. 2. (a) Refractive indices and (b) extinction coefficients of the ITO films deposited with different oxygen flow rate.

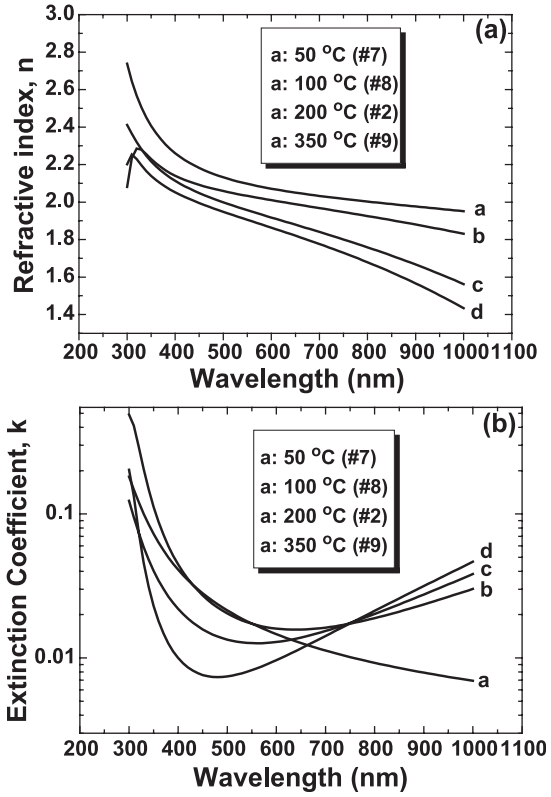

Fig. 3. (a) Refractive indices and (b) extinction coefficients of the ITO films deposited at different temperatures.

Higher deposition temperatures resulted in lower refractive indices. The changes in extinction coefficients are quite different between the visible range (about 400–700 nm) and the near infrared region (above 700 nm). In the visible range, the extinction coefficients were lower for higher deposition temperature conditions. However, in the near infrared region, higher deposition temperature led to larger extinction coefficients. Table 1 exhibits that the ITO films with higher deposition temperature have higher electron concentration and lower relative intensity of (222)-peak (sample numbers 2, 7, 8, and 9). Also, the ITO films were denser when deposited at higher temperatures.

Fig. 4 shows the spectra of refractive indices and extinction coefficients of the ITO films deposited with different sputtering pressure (sample numbers 1, 3, and 4). The films were deposited at 200 °C without supplying additional oxygen gas. In the moderate range of sputtering pressure (about 0.7 Pa in this research), the ITO films have lower optical constants (both n and k values). As shown in Table 1, in the pressure range, the ITO films were denser, and the relative intensity of (222)-peak was lower. Also, carrier density was relatively higher for the moderate range of sputtering pressure.

In many cases, the relationships between the optical constants and the microstructure of transparent oxide films are explained from a linear law of mixing [16,17];

$$n_f = n_b P + n_v(1 - P) \quad (2)$$

where n_f, n_b, and n_v are the refractive indices of film, bulk, and void, and P represents the packing fraction of films, respectively. Thus, many researchers have reported larger optical constants for denser film structure of metallic oxides [18–20]. However, in this research, higher optical constants were not acquired for the samples deposited under the conditions for higher film density. In Fig. 2, the sample of lowest film density (sample number 4, no oxygen) shows lowest refractive indices. However, the highest film density (sample number 5, oxygen 1 sccm) does not correspond to highest refractive indices (sample number 6, oxygen 3 sccm). Similar results were reported by other researchers [10]. Moreover, as shown in Figs. 3 and 4 and Table 1, denser ITO samples have lower refractive indices. These results mean that there are more decisive factors controlling the refractive indices of ITO thin films.

On the other hand, crystallographic orientation of the ITO films showed a clear relationship with refractive indices. More (222) orientation of the samples resulted in higher refractive indices. Many researchers have reported the change of crystallographic orientations of ITO films with different sputtering conditions [21–24].

Many crystalline materials are optically anisotropic since the binding forces on the electrons would be different depending upon directions due to asymmetric atomic

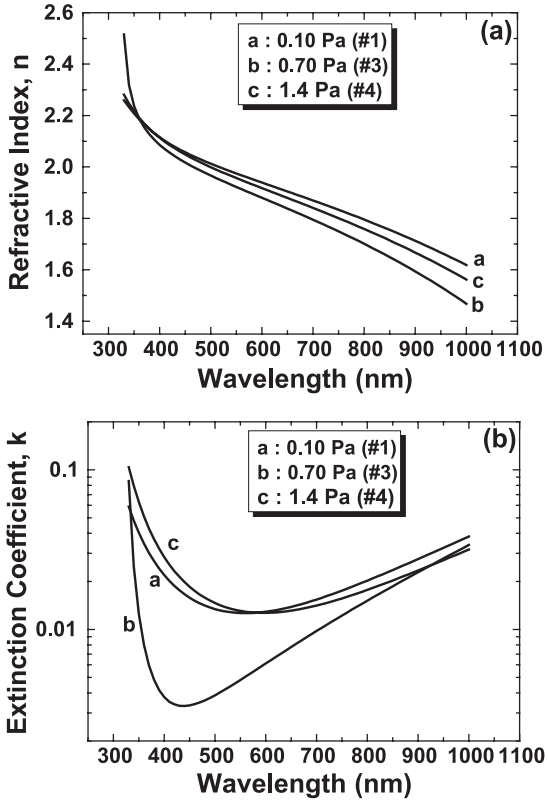

Fig. 4. (a) Refractive indices and (b) extinction coefficients of the ITO films deposited under different sputtering pressure.

arrangement. Crystalline materials with cubic structures are usually optically isotropic. In most cases, ITO films crystallize in a cubic bixbyite structure [25,26]. Accordingly, any perpendicular crystallographic planes in ITO films would have an optical symmetry with each other. However, (222) planes and (400) planes, which are the main crystallographic orientations of the ITO thin films prepared in this research, are not perpendicular. If there were the ITO films with a prefect (222) or a (400) orientation to the substrates, they would have different optical constants in the perpendicular direction to substrates as a result of different oscillator energies of electrons due to different atomic arrangement. For all the samples shown in Figs. 2–4 and Table 1, the higher portion of (222) orientation of the samples seems to be closely related with higher refractive indices, in spite of lower film density.

The changes in extinction coefficients are quite different between the visible range and the near infrared region. In the visible range, higher extinction coefficients can be originated from sub-oxide phases such as InO_x or SnO_x or crystallographic flaws such as grain boundaries and voids. Sub-oxide phases act as optical scattering centers [27]. The non-stoichiometric sub-oxide phases are expected to be formed due to oxygen deficiency or low crystallinity. In Fig. 2(b), the sample deposited with no oxygen gas showed relatively higher extinction coefficients. Slightly higher extinction coefficients for 3 sccm than those for 1 sccm may be resulted from lower crystallinity. With increased oxygen partial pressure during sputtering, more oxygen atoms would be absorbed on the substrate or the film surface. Accordingly, the In and Sn metal adatoms are likely to be easily trapped by the oxygen atoms [20]. Thus, the average mobility and diffusion length of adatoms will decrease under the conditions of high oxygen partial pressure, and, consequently, the films would have low crystallinity when deposited with excessively high oxygen gas. Higher extinction coefficients in the near infrared range for the sample with lower oxygen flow rate are due to higher carrier concentration originating from higher number of oxygen vacancies in the film.

Higher deposition temperature resulted in lower extinction coefficients in the visible range, as shown in Fig. 3(b). This is apparently due to better crystallinity of the samples. On the other hand, in the near infrared region, higher temperature caused higher extinction coefficients. Higher carrier density of the samples is expected to lead to higher optical scattering and absorption in the spectral range.

Moderate range of sputtering pressure results in lower extinction coefficients as shown in Fig. 4(b). At very low pressure (about 0.1 Pa), adatom mobility will be low in spite

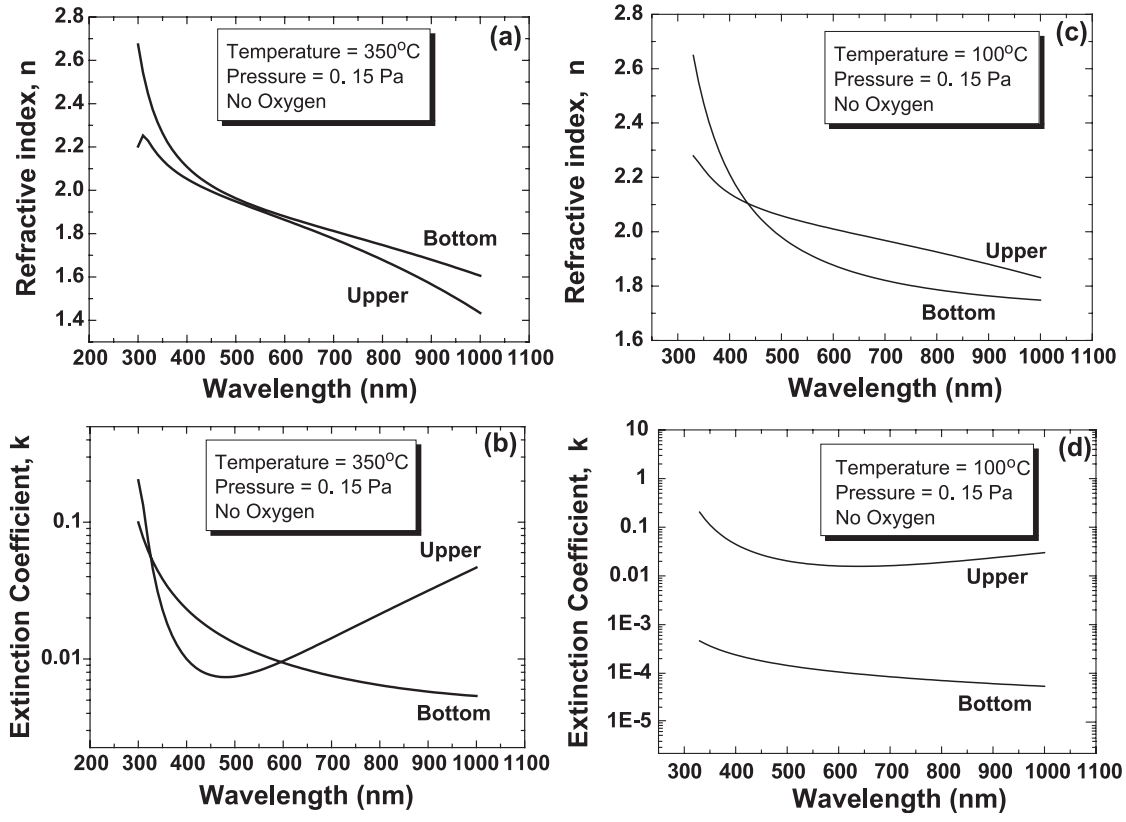

Fig. 5. (a) Refractive indices and (b) extinction coefficients of the upper and the bottom ITO layers (mixed orientation). (c) Refractive indices and (d) extinction coefficients of the upper and bottom ITO layers (perfect (222) orientation).

of relatively higher ion energy because of very low ion density. On the other hand, at very high pressure (about 1.4 Pa), lower ion energy as a result of frequent collision among neutral gases and ions results in very low adatom mobility. Consequently, crystallinity seems to be better in the moderate range of pressure (about 0.7 Pa in this research), where the adatom mobility is expected to be highest. The extinction coefficients in the near infrared region are similar among the samples, however, if the measurement were conducted through longer wavelength range, the sample deposited at 0.70 Pa would have higher extinction coefficients. Actually, the extinction coefficient of the sample increases most rapidly in the near infrared region, as shown in Fig. 4(b).

ITO thin films generally contain graded properties since the initial layers of films usually have heavily disordered microstructures. It is especially important when characterizing the optical and electrical properties of transparent conducting oxides since free carriers are distributed inhomogeneously. Fig. 5(a) presents the difference in optical constants between the upper and the bottom layers. The sample (number 9) was deposited without additional oxygen gas. As shown in Fig. 5(a), refractive indices were similar or slightly higher for the bottom layer. R.A. Synowicki reported similar results [7]. In contrast, Fig. 5(c) shows quite different phenomena. As for the sample (number 7), upper layer has higher refractive indices. Many researchers also reported these results, and attributed the phenomena to less dense structure of initial layers [5,8]. These results seem to be pretty inconsistent, but the data shown here was reproducible. The samples with a perfect (222) orientation (sample numbers 6, 7, and 8) had higher refractive indices at the upper layers, as shown in Fig. 5(c). In contrast, for the ITO films with mixed orientations, the bottom layers had higher refractive indices.

Fig. 6 shows the XRD patterns of the ITO samples with different thickness. The ITO samples were deposited at 200 °C without supplying additional oxygen gas. The ITO samples deposited under this condition had mixed orientations. The graphs present that the sample with higher thickness has higher portion of (400)-oriented grains. That means that upper layers have higher portion of (400)-oriented grains. As previously mentioned in this research, more (400) orientation resulted in lower refractive indices. Thus, in spite of higher film density, the upper layers have lower refractive indices in the cases of mixed orientations. However, in the cases of a perfect (222) orientation, there are no differences in crystallographic orientation between the upper and the bottom layers, thus, film density governs refractive indices, which means higher film density at the upper layers.

Higher free carrier density due to better crystallinity and higher film density at the upper layer seem to be responsible for higher extinction coefficients in the near infrared region as shown in Fig. 5(b). Exceptionally low extinction coefficients in the bottom layer in Fig. 5(d) seem to be resulted from extremely low free carriers.

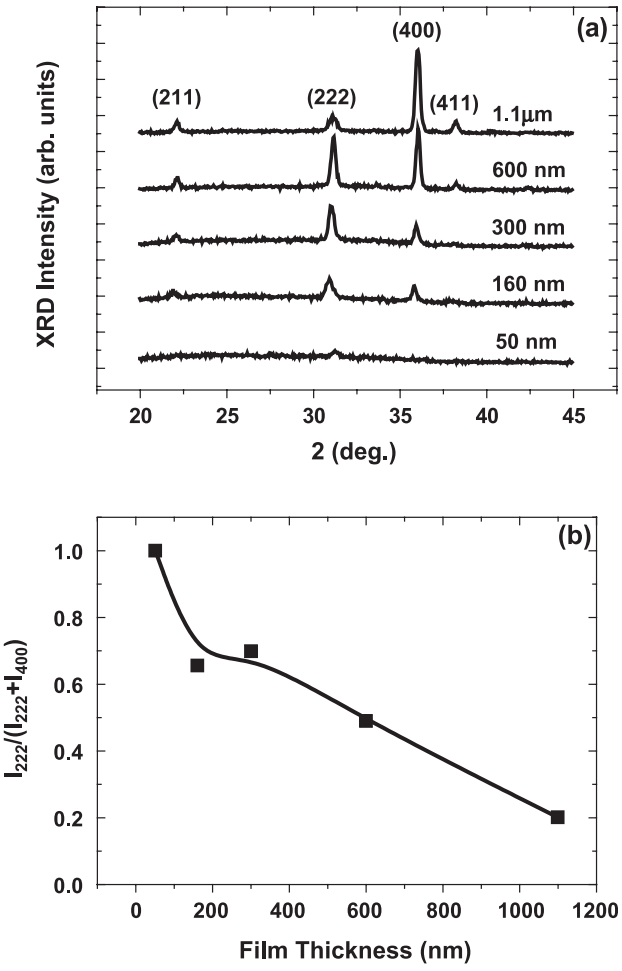

Fig. 6. Change of (a) XRD diffractograms and (b) $(I_{(222)}/(I_{(222)}+I_{(400)}))$ depending upon film thickness.

4. Conclusions

ITO thin film samples were prepared under various DC magnetron sputtering conditions. The optical constants of ITO films were analyzed based on a model combining a Drude absorption edge and Lorentz oscillators. To analyze the graded structure of the films, two independent layers were used. Lower amount of oxygen flow, moderate range of sputtering pressure, and higher deposition temperature resulted in lower refractive indices. These results were explained from different crystallographic orientations. The samples with higher refractive indices had more (222)-oriented crystallographic structures. Different crystallinity, stoichiometry, and carrier concentration were responsible for the change of extinction coefficients. Also, the variations in refractive indices between the bottom and upper layers

were explained from graded crystallographic orientation based on XRD analyses.

References

[1] G. Haacke, Annu. Rev. Mater. Sci. 7 (1977) 73.
[2] C.G. Grandqvist, Appl. Phys., A Mater. Sci. Process. 52 (1991) 83.
[3] A.K. Kulkarni, K.H. Schulz, T.S. Lim, M. Khan, Thin Solid Films 345 (1999) 273.
[4] J.A. Woollam, W.A. McGahan, B. Johs, Thin Solid Films 241 (1994) 44.
[5] J.N. Hilfiker, R.A. Synowicki, J.S. Hale, C. Bungay, Society of Information Display, Digest of Technical Papers, San Diego, 2002, p. 491.
[6] H.E. Rhaleb, E. Benamar, M. Rami, J.P. Roger, A. Hakam, A. Ennaoui, Appl. Surf. Sci. 201 (2002) 138.
[7] R.A. Synowicki, Thin Solid Films 313–314 (1998) 394.
[8] M. Losurdo, D. Barreca, P. Capezzuto, G. Bruno, E. Tondello, Surf. Coat. Technol. 151–152 (2002) 2.
[9] M. Losurdo, M. Giangregorio, P. Capezzuto, G. Bruno, R.D. Rosa, F. Roca, C. Summonte, J. Pia, R. Rizzoli, J. Vac. Sci. Technol., A, Vac. Surf. Films 20 (2002) 37.
[10] L.J. Meng, E. Crossan, A. Voronov, F. Placido, Thin Solid Films 422 (2002) 80.
[11] D.A.G. Bruggeman, Ann. Phys. 24 (1935) 636.
[12] P.K. Song, Y. Shigesato, I. Yasui, C.W. Ow-Yang, D.C. Paine, Jpn. J. Appl. Phys. 37 (1998) 1870.
[13] J. Kanazawa, T. Haranoh, K. Matsumoto, Vacuum 41 (1990) 1463.
[14] T. Minami, H. Sonohara, T. Kakumu, S. Takata, Thin Solid Films 270 (1995) 37.
[15] W. Fukarek, H. Kersten, J. Vac. Sci. Technol., A, Vac. Surf. Films 12 (1994) 523.
[16] M. Harris, H.A. Macleod, S. Ogura, E. Pelletier, B. Vidal, Thin Solid Films 57 (1979) 173.
[17] M. Ohring, The Materials Science of Thin Films, Academic Press, Boston, 1992.
[18] C.C. Lee, J.C. Hsu, D.H. Wong, Appl. Surf. Sci. 171 (2001) 151.
[19] S.B. Amor, G. Baud, J.P. Besse, M. Jacquet, Mat. Sci. Eng. B 47 (1997) 110.
[20] B. Hunche, M. Vergohl, H. Neuhauser, F. Lose, B. Szyszka, T. Matthee, Thin Solid Films 392 (2001) 184.
[21] P.K. Song, Y. Shigesato, M. Kamei, I. Yasui, Jpn. J. Appl. Phys. 38 (1999) 2921.
[22] H. Izumi, F.O. Adurodija, T. Kaneyoshi, T. Ishihara, H. Yoshioka, M. Motoyama, J. Appl. Phys. 91 (2002) 1213.
[23] F.E. Akkad, M. Marafi, A. Punnoose, G. Prabu, Phys. Status Solidi, A Appl. Res. 177 (2000) 445.
[24] P.K. Song, Y. Shigesato, I. Yasui, C.W. Ow-Yang, D. Paine, Jpn. J. Appl. Phys. 37 (1998) 1870.
[25] M. Marezio, Acta Crystallogr. 20 (1966) 723.
[26] A. Gurlo, M. Ivanovskaya, N. Barsan, U. Weimar, Inorg. Chem. Commun. 6 (2003) 569.
[27] Y. Shigesato, D.C. Paine, T.E. Haynes, Jpn. J. Appl. Phys. 32 (1993) L1352.